Research of particularities in formation of microstructures, mechanic and electric properties of lithium niobate ceramics in dependence to the initial charge dispersity

UDC 537.9+537.312.6+542.86+544.032.4

M. N. Palatnikov, *Sector Leader*[1]
O. B. Shcherbina, *Senior Researcher*[1], *e-mail: shcerbina@chemy.kolasc.net.ru*
S. M. Masloboeva, *Assistant Professor*[1]
V. V. Efremov, *Senior Researcher*[1]

[1] *I. V. Tananaev Institute of Chemistry and Technology of Rare Elements and Mineral Raw Material KSC RAS, Apatity, Russia.*

The structure, mechanic and electric properties were researched in ceramics obtained on the basis of highly disperse microcrystal single phase powders of lithium niobate. Methods of research were probe microscopy and impedance spectroscopy. The distribution of powder particles sizes was narrow. The ceramic materials properties was shown to depend on dispersity of the initial powder lithium niobate charge. At this, due to formation of gradient mezostructure in LN ceramic obtained from initial charge with low specific surface area microhardness measured on the surface of this sample was almost equal to the one of samples more homogeneous in size grains and more dense synthesized from charge with higher specific surface area. At the same time Young modulus that is a strength index of the material, is naturally higher for LN ceramic samples obtained from charge with higher specific surface area. Great differences in ceramic structure on mezo- and microlevels manifest in mechanical properties especially in the destruction processes and strength. The criterion for evaluation of plastic and brittle properties was chosen micro-brittleness and brittle microstrength. The obtained data allowed us to evaluate critical stress intensity factor of the first kind K_{IC} which is a material crack-resistance criterion. Crack-resistance and microhardness of the materials were shown to increase with increase in the dispersity of the initial charge. The dispersity of complex impedance $Z^*(\omega)$ was researches for the most dense LN ceramic sample in the temperature range up to ~800 K. Real and imaginary components of the complex dielectric permittivity and complex impedance (admittance) were detected due to measured real value of impedance (Z) and phase difference angle (φ). Temperature dependence of static conductivity $\sigma_{sv}(T)$ of LN ceramic agrees with the Arrhenius law only in high-temperature area. The dependence has a monotonous shape with activation enthalpy $H_a \approx 0.88$ eV. Such value is typical for the ion conductivity along the ceramic grain boarders. Comparison of the specific static conductivity of ceramic and crystals LN samples revealed that ceramic conductivity is four times of magnitude higher σ_{sv} ~$5.0 \cdot 10^{-8}$ S/m and $5.0 \cdot 10^{-12}$ S/m, correspondingly.

Key words: lithium niobate, dispersity, ceramics, microhardness, Yong modulus, mechanical and electrophysical properties.

DOI: *10.17580/nfm.2017.01.01*

Introduction

Lithium niobate (LN, $LiNbO_3$) is one of the basic materials of microelectronic. LN has important practical applications not only in single crystal but also in disperse condition, and as ceramic functional material. Detectors of ionizing radiation, sensors, micro- and nanoelectromechanical systems (MEMS/NEMS), actuators working on piezoelectric or electret effects could be created on the base of high-density piezo-ferroelectric ceramics obtained from micro- and nanocrystal LN powders [1]. Thus research of patterns of LN properties changes in disperse or ceramic condition is essential and relevant.

Experiment

We used fluoride niobium containing solution (Nb_2O_5 – 127.4, F – 132.3 g/l) to obtain microcrystal LN powders. Due to mass spectrometric analysis with inductively coupled plasma the solution contained microimpurities Mg, Al, Ti, Fe, Cu, Pb, Sn, Ni, Cr, Co $(1–2) \cdot 10^{-4}$ g/l or less, Ta – 0.008 g/l. The powders synthesis was performed in one technologycal cycle due to [2]. We added 25% NH_4OH solution (contained less than 10^{-6} % (mol.) impurities) until pH reached 8–9 to precipitate niobium hydroxide. We vacuum-filtered the sediment and washed it threefold by repulpation in deionized water. The solid-liquid phases ratio was $S{:}V_1 = 1{:}2$. We did it to dispose of

ammonium and fluorine ions. We mixed wet (~65%) clear niobium hydroxide with lithium acetate ($Li(CH_3COO)$) solution at $S:V_l = 1:1$ for 3 h. We evaporated the pulp to a viscous condition, dried at 140 °C. The residual was heated at 1100 °C for 6 h. We prepared $Li(CH_3COO)$ from lithium carbonate Li_2CO_3 (10^{-4} admixtures and less) and acetic acid solution. Li concentration corresponded to molar ratio [Li]/[Nb] = 1.04.

The *X*-ray analyses were carried out on diffractometer DRON-2, the counter speed was 2 angles per minute, CuK_α-radiation and graphite monochromator were used. The phase identification was carried out due to data base JCPDS, card 88-0289. The results confirmed obtaining of single phase product in the given conditions.

Nb concentration in the LN powder was 62.07% (wt.) due to chemical analysis. Li concentration (4.9% (wt.)) was detected by mass spectrometric analysis with inductively coupled plasma. The data correlate with the chosen molar ratio [Li]/[Nb].

The LN powder was detected to be conglomerates. The latter consist of crystal particles of different sizes with difficult surface. Flattened facetedness with indistinct manifestation of habitus is typical for the conglomerates. The destruction of the conglomerates was carried out. The LN powder (charge) was milled. After that the result was separated into narrow granule fractions by decantation [3]. The specific surface of the powders was detected by low-temperature nitrogen adsorption (BET; FlowSorbII 2300; TriStar 3020 V1. 03). Table 1 shows the specific surface of the LN powders. Values of S_{sp} for the decantated fractions is much higher (2–3 times) than for the initial powders. Annealing kinetics, homogeneity, mezostructure and properties of the ceramic samples prepared from more disperse powders should change due to increase in specific reaction ability of charge particles.

Four samples (1–4) were prepared from LN charge with different dispersity due to conventional technology [4] (see Table 1). Annealing temperature was ~1100 °C, heating velocity was 100 °C/h, time of the heating at the maximum temperature was ~3 h.

Ceramic samples mezostucture was researched by optical method. We used scanning electron microscope SEM LEO 420 to research micro- and mezostructure of the samples and software Scan Master for analysis and mathematical treatment of the scanned images.

Mechanical properties were researched by probe method at probe microscope – nanohardness-meter NANOSKAN.

Micro-brittleness was detected due to formula $\gamma = (L^2 - l^2)/l^2$, where l is a scratch wideness measured between the walls, μm; L — size of the brittle damage zone (including all distortions of the surface solid, such as cracks, chips, etc. [5]) in the area of the indenter influence, μm. The brittle damage zone was evaluated due to the maximum damage of the researched scratch, regardless of the direction. Such evaluation is justified because the crack continues until the tension on its end is equal to the strength limit of the tested material. Microhardness was calculated due to formula $\sigma = P/L^2$.

Platinum electrodes were magnetron sputtered on ceramic LN samples (~10 mm in diameter and 1.5 mm thick) to research their dielectric properties. Measurements were carried out on Solartron 1260 in the frequency range 1 Hz – 1 MHz during stepwise heating mode. This method enables separation of contributions of various relaxation processes to the measured values and correct calculation of the static specific conductivity [6–8].

Results and discussion

Mezo- and microstructure of sample 1 is different from other samples (2–4) (Fig. 1). Sample 1 structure is highly inhomogeneous. It contains both large grains ~40 μm and microcrystals 2 μm (Fig. 1, *a*, *c*). Boarders of large grains contain cracks and voids. LN ceramic samples obtained from the dispersed charge (samples 2–4) are more homogeneous (Fig. 1, *b*). The differential distribution curves (Fig. 1, *b*, *d*) show that most microcrystals of the ceramic are close to the nanometer diapason boarder. Microcrystals have size ~0.2–2.0 μm. At this adhesive ability of ceramic grains obviously rises, the ceramic is more durable and has a significant microhardness.

The results of measurements of the microhardness by comparative sclerometry [6] and Young modulus by the approach curves is demonstrated in Table 2. Calculations were carried out due to the model for the case of the indentation by the Vickers pyramid [5].

Surface microhardnes of sample 1 is comparable with more dense samples 2–4 due to formation of the gradient microstructure expressed in the form of individual large crystallites. However the Young modulus value is obviously higher for samples 2–4, because this value is a strength index of the material.

The differences in ceramics mezo- and microstructure should reveal in the mechanical characteristics, i. e. destruction processes and strength. Micro-brittleness and brittle micro-strength are evaluation criterions for plastic and brittle properties of materials. The obtained data let us estimate the critical stress intensity factor of the first

Table 1

Specific surface of different LN charge

Charge particle size $LiNbO_3$, μm	Initial powder, 50–140	5–10	<5	<3
Specific surface S_{sp}, m^2/g	0.07	2.27	4.67	5.26
Sample	1	2	3	4

Table 2

Microhardness and Young modulus of the LN ceramic samples obtained from charge of different dispersity

$LiNbO_3$ samples	1	2	3	4
Microhardness *H*, GPa, average	5.46±1.55	5.52±1.02	4.6±1.41	5.0±2.17
Young modulus *E*, GPa	146.7±5.0	146.0±4.8	235.1±9.2	188.7±2.9

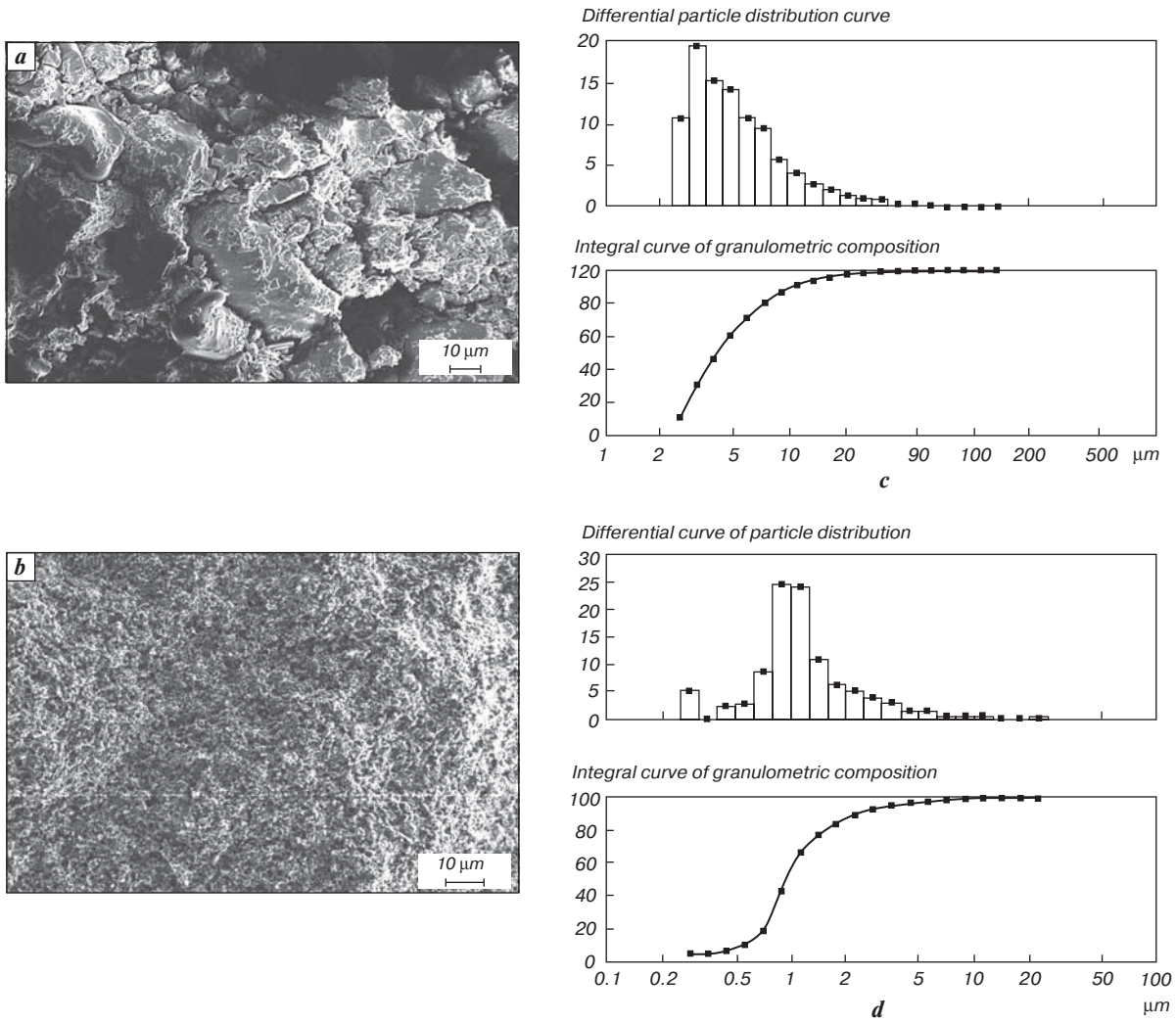

Fig. 1. Structure and size compound of LN ceramic samples obtained from the charge of different dispersity: *a*, *c* — sample 1; *b*, *d* — sample 4

kind K_{IC}. This factor is a criterion of the material crack resistance [5, 6]. Mechanical characteristics of LN ceramic samples are demonstrated in Table 3. The table shows that LN ceramic samples obtained from dispersed charge (sample 2, 3, 4) have much higher crack resistance and microhardness than the ceramics obtained from the initial powder (charge 1).

Composite impedance variance $Z^*(\omega)$ is researched in this paper for LN ceramic samples in the temperature range up to ~800 K. Real and imaginary components of the complex dielectric permittivity and complex impedance (admittance) were detected due to measured Z and φ values.

$Z'' - Z'$ diagrams are qualitatively similar for all researched LN ceramic samples (1–4) in the whole temperature range. They reveal one relaxation process as an arc of a circle. Fig. 2, *a–c* demonstrates diagrams of complex impedance for the densest ceramic sample (4) obtained at temperatures: *a* — 289 K, *b* — 374 K, *c* — 791 K.

The value of the static conductivity of the sample volume ($\omega \to 0$) could be separated from the impedance hodographs by excluding the polarization of electrodes.

Table 3

Mechanical characteristics in dependence of stress of LN ceramic samples obtained from charge of different dispersity

$LiNbO_3$ ceramic	1			2			3			4		
Stress *P*, MN	10	15	20	10	15	20	10	15	20	10	15	20
Micro-brittleness γ	0.55	0.63	0.65	0.37	0.39	0.39	0.35	0.41	0.39	0.28	0.36	0.32
Fragile micro-strength, GPa	1.14	1.0	0.98	1.33	1.40	1.57	1.63	1.39	1.43	1.47	1.68	1.68
Crack resistance K_{IC}, MPa/m^2	1.03	1.33	1.22	1.60	1.6	1.91	1.66	1.65	1.72	1.9	2.02	2.01

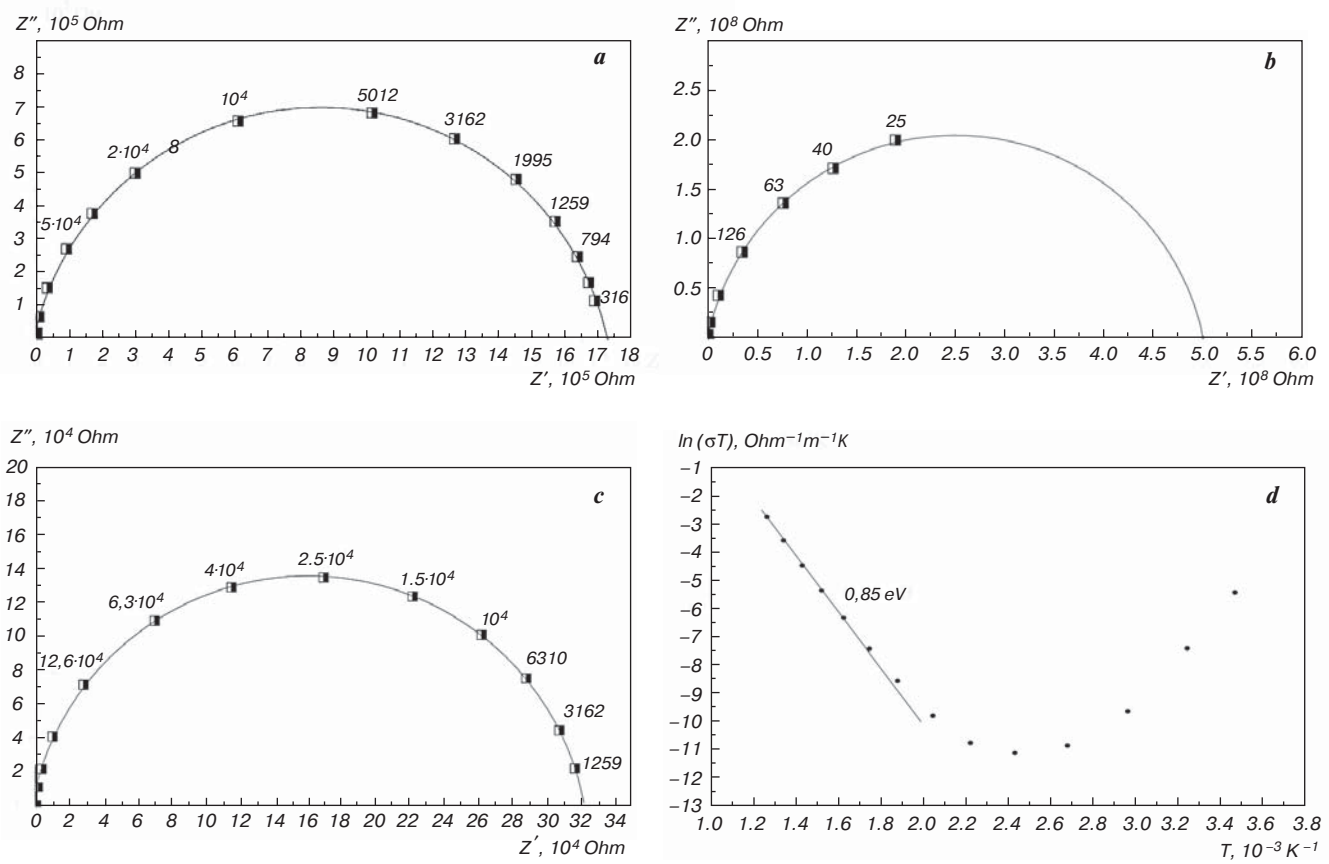

Fig. 2. Diagrams of complex impedance (frequencies are in Hz) for the densest LN ceramic sample 4, obtained at: *a* — 289 K; *b* — 374 K; *c* — 791 K; and temperature dependence of the specific conductivity (*d*) of the sample

High specific conductivity of the sample is obvious even at room temperature. The sample static conductivity is $\sigma_{sv} \sim 1.475 \cdot 10^{-5}$ S/m at 289 K. Rise in temperature leads to decrease in static conductivity. Fig. 2, *b* demonstrates that static conductivity of sample 4 at 374 K decreases to value $\sigma_{sv} \sim 5.09 \cdot 10^{-8}$ S/m. This trend continues to the temperature 412 K. At higher temperatures static conductivity starts to increase. Fig. 2, *c* was obtained at 791 K. It demonstrates that static conductivity of the ceramic LN increases to $\sigma_{sv} \sim 7.914 \cdot 10^{-5}$ S/m.

Temperature dependence of static conductivity is demonstrated on Fig. 2, *d*. The figure shows that $\sigma_{sv}(T)$ agrees with the Arrhenius law only in high-temperature area. The dependence has a monotonous shape with activation enthalpy $H_a \approx 0.88$ eV. Such value is typical for the ion conductivity along the ceramic grain boarders. Low-temperature area is different. High static conductivity values at room temperature and its decrease with the rise in temperature is apparently connected with adsorbed water in the sample. Thus high sample humidity makes the predominant contribution to the electrical conductivity at low temperatures, not intrinsic conductivity. Desorption of water occurs with rise in temperature thus LN ceramic samples conductivity decreases.

Fig. 3 demonstrates temperature dependence of real part of dielectric permittivity in LN ceramic sample 4. Dielectric permittivity dispersion at low temperatures is apparently connected with high sample humidity. In the temperature range 350–650 K dielectric permittivity

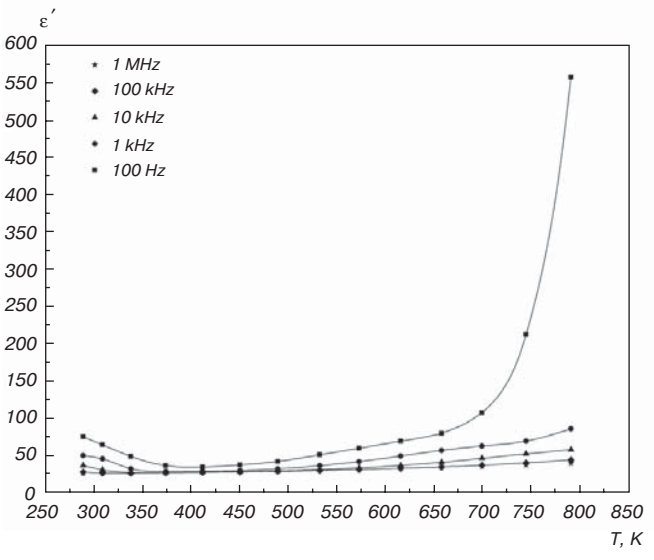

Fig. 3. Temperature dependence of real part of dielectric permittivity in LN ceramic sample 4 at different frequencies

of sample 4 is much lower than in other ferroelectrics. Dielectric dispersion begins only after ~700 K.

Specific static conductivity is much lower for LN congruent single crystal than for the ceramic samples [9–14]. Specific static conductivity of LN ceramic sample 4 is ~$5.0 \cdot 10^{-8}$ S/m, at temperatures higher than ~400 K when water desorbs. At the same time this value is four orders of magnitude higher than for LN congruent single crystal (σ_{sv} ~ $5.0 \cdot 10^{-12}$ S/m) [9] at the same temperature.

Activation enthalpy of static conductivity for ceramic LN at temperatures $T \geq 550$ K ($H_a \approx 0.88$ eV) is lower than for single crystal sample in the area of Li conductivity ($T \geq 550$ K) $H_a \approx 1.25$ eV [9, 10]. It could be explained by the fact that ceramic LN being a poly-crystal possesses great amount of grains and system of intergranular boundaries with a large number of intergranular defects (i. e. structure vacancies).

In the ceramics the ion conductivity is not bulk (as in single crystal), but along the grain boundaries. The latter increases due to appearance of conductivity ions connected with crystal latter defects on the grains boundaries. Thus polycrystal ceramic sample has higher ion conductivity in comparison with the single crystal sample.

Conclusions

Research of LN ceramic samples obtained on the base of single crystal powders of different dispersity with narrow particles sizes distribution has demonstrated the possibility to control both structure ceramic forming and number of physical characteristics by change of lithium niobate charge dispersity.

References

1. Kühler M., Fritzsche W. Nanotechnology: An Introduction to Nanostructuring Techniques. Weinheim : Wiley-VCH. 2004. pp. 27–28.

2. Masloboeva S. M., Palatnikov M. N., Arutunjan L. G. et al. Obtaining and investigation of microcrystalline powders of lithium niobate and tantalate. *Collection of scientific proceedings "Physical and chemical aspects of investigation of clusters, nanostructures and nanomaterials"*. Tver : Tverskoy Gosudarstvennyy universitet. 2016. Iss. 8. pp. 239–246.

3. Bulanov V. Ya., Kvater L. I., Dolgal T. V. et al. Metallic powder diagnostics. Moscow : Nauka, 1983. 280 p.

4. Palatnikov M. N., Sidorov N. V., Kalinnikov V. T. Segnetoelectric solid solutions based in oxide compounds of niobium and tantalum. Saint Petersburg : Nauka. 2002. 304 p.

5. Oliver W. C., Pharr G. M. An Improved Technique for Determining Hardness and Elastic Modulus Using Load and Displacement Sensing Indentation Experiments. *Journal of Materials Research*. 1992. Vol. 7. pp. 1564–1583.

6. Useinov A. S. A Nanoindentation Method for Measuring the Young Modulus of Superhard Materials Using a NanoScan Scanning Probe Microscope. *Pribory i tekhnika eksperimenta*. 2004. No. 1. pp. 134–138.

7. Tsai Y.-T., Whitmore D. H. Nonlinear Least-Squares Analyses of Complex Impedance and Admittance Data for Solid Electrolytes. *Solid State Ionics*. 1982. Vol. 7. pp. 129–139.

8. Jonscher A. K. Dielectric Relaxation in Solids. Chelsea Dielectrics Press. London. 1983. 380 p.

9. Yatsenko A. V., Palatnikov M. N., Sidorov N. V., Pritulenko A. S., Evdokimov S. V. Specific features of electrical conductivity of $LiTaO_3$ and $LiNbO_3$ crystals in the temperature range of 290–450 K. *Physics of the Solid State*. 2015. Vol. 57, No. 8. pp. 1547–1550.

10. Akhmadullin I. Sh., Golenishchev-Kutuzov V. A., Migachev S. A. et al. Low-temperature electrical conductivity of congruent lithium niobate crystals. *Physics of the Solid state*. 1998. Vol. 40, No. 7. pp. 1190–1192.

11. Rahn J., Hüger E., Dörrer L., Ruprecht B., Heitjans P., Schmidt H. Li self-diffusion in lithium niobate single crystals at low temperatures. *Physical Chemistry Chemical Physics*. 2012. Vol. 14. pp. 2427–2433.

12. Fielitz P., Borchardt G., Ganschow S., Bertram R., Jackson R., Fritze H., Becker K. Tantalum and niobium diffusion in single crystalline lithium niobate. *Solid State Ionics*. 2014. Vol. 259. pp. 14–20.

13. Shi J., Fritze H., Weidenfelder A., Swanson C., Fielitz P., Borchardt G., Becker K. Optical absorption of electronic defects and chemical diffusion in vapor transport equilibrated lithium niobate at high temperatures. *Solid State Ionics*. 2014. Vol. 262. pp. 904–907.

14. Weidenfelder A., Fritze H., Fielitz P., Borchardt G., Shi J., Becker K., Ganschow S. Transport and Electromechanical Properties of Stoichiometric Lithium Niobate at High Temperatures. *Zeitschrift für Physikalische Chemie*. 2012. Vol. 226. pp. 421–428.

NFM